

# Online Particle Smoothing with Application to Map-matching

Samuel Duffield\*, Sumeetpal S. Singh

Department of Engineering, University of Cambridge

December 2020

## Abstract

We introduce a novel method for online smoothing in state-space models based on a fixed-lag approximation. Unlike classical fixed-lag smoothing we approximate the joint posterior distribution rather than just the marginals. By only partially resampling particles, our online particle smoothing technique avoids path degeneracy as the length of the state-space model increases.

We demonstrate the utility of our method in the context of map-matching, the task of inferring a vehicle’s trajectory given a road network and noisy GPS observations.

## 1 Introduction

Widely used in modelling dynamical systems and time series, a state-space model is fully defined by the following distributions for the hidden  $\{x_t\}_{t=0}^{\infty}$  and observed process  $\{y_t\}_{t=0}^{\infty}$

$$\begin{aligned} p(x_0), \\ p(x_t|x_{t-1}), & \quad t = 1, 2, 3, \dots \\ p(y_t|x_t), & \quad t = 0, 1, 2, \dots \end{aligned}$$

The statistical inference goal of *smoothing* is the task of approximating the full joint posterior or smoothing distribution

$$p(x_{0:T}|y_{0:T}) \propto p(x_0|y_0) \prod_{t=1}^T p(x_t|x_{t-1})p(y_t|x_t), \quad (1)$$

where  $x_{0:T} = (x_0, \dots, x_T)$  are latent states to be inferred and  $y_{0:T} = (y_0, \dots, y_T)$  are given observations.

For *online smoothing*, we have the additional requirement of being able to quickly and accurately update an approximation of  $p(x_{0:T-1}|y_{0:T-1})$  to approximate  $p(x_{0:T}|y_{0:T})$  in light of receiving a new observation  $y_T$ .

A popular and powerful approach to inference in general state-space models is that of particle filtering/smoothing (or sequential Monte Carlo) [1–3]. Particle smoothers approximate (1) with a collection of weighted (or unweighted) particles

$$p(x_{0:T}|y_{0:T}) \approx \sum_{i=1}^N w_T^{(i)} \delta_{x_{0:T}} \left( x_{0:T}^{(i)} \right),$$

---

\*Corresponding author: sddd2@cam.ac.uk, Samuel Duffield is supported by the EPSRC

as opposed to particle filters which are only required to approximate  $p(x_T|y_{0:T})$ . Existing online particle smoothing approximations either degenerate as the length of the state-space model,  $T$ , increases or only target the smoothing marginals  $p(x_t|y_{0:T})$  rather than the joint smoothing distribution. A particle approximation to the joint smoothing distribution is significantly more useful as mathematical expectations can be calculated over a range of functions defined over full trajectories, thus providing the user with complete flexibility.

In summary, our motivation is to develop an algorithm that simultaneously satisfies the following requirements

- (R1) **Joint Smoothing:** The algorithm efficiently approximates the joint posterior  $p(x_{0:T}|y_{0:T})$  rather than only marginals.
- (R2) **Online:** Our approximation can be quickly updated as it receives new observations.
- (R3) **Non-degenerate:** The algorithm doesn't suffer from the path degeneracy of classical particle filters.

In particular, we are interested in the application of particle smoothing to urban map-matching. The combination of dense road networks (with frequent intersections) and noisy GPS observations leads to uncertainty over the location and route of vehicles. This is a particularly compelling application of online joint smoothing where it is desirable to represent the route with particles that each describe a complete vehicle trajectory.

The contribution of this work is to introduce two general techniques for generating samples on-the-fly that approximate the joint smoothing distribution (1) via a fixed-lag approximation. We also formulate a robust state-space model for urban map-matching before describing and implementing both offline and online particle smoothing efficiently in this context.

The rest of the paper is structured as follows. In Section 2 we discuss related online and offline algorithms for particle smoothing, as summarised in Table 1 alongside those introduced in this paper. Section 3 describes how to combine samples in a way that is invariant for a fixed-lag joint smoothing distribution and Section 4 introduces two efficient online methods for generating these samples. Section 5 describes the problem of map-matching and Section 6 demonstrates numerically the benefits of uncertainty quantification as well as the performance of the introduced online particle smoothers and their sensitivity to key parameters. In Section 7 we conclude and discuss some potential extensions.

## 2 Background and Related Work

### 2.1 Particle Filtering and Path Degeneracy

A classical particle filter runs a single forward pass, updating particles at every observation. Each update consists of three steps: an optional *resample* step, a *propagation* step and a *weighting* step. These steps are described in Algorithm 1.

The resampling operation converts a weighted sample into an unweighted sample that likely contains duplicates, most commonly via multinomial sampling (with replacement). Due to the optional nature of the resampling step, adaptive schemes are often applied, with a popular choice to be to only resample if the effective sample size  $1/\sum_{i=1}^N w_T^{(i)2}$  falls below some threshold.

Although most commonly only used only to approximate the filtering marginals  $p(x_T|y_{0:T})$ , the particle filter as described in Algorithm 1 does provide an asymptotically unbiased approximation to the full smoothing distribution  $p(x_{0:T}|y_{0:T})$ .

	Joint Smoothing	Online	Path Degeneracy	Fixed-lag Approx.	Complexity
Particle Filter [1]	✓	✓	✓		$N$
Marginal Fixed-lag [4]		✓	For large $L$	✓	$N$
Forward Filtering-Backward Smoothing [5]					$N^2$
Forward filtering-Backward Simulation [6]	✓				$N^2$ $N$ with RS <sup>†</sup>
Forward Filtering-Backward Smoothing for Additive Functionals [7]		✓			$N^2$
PaRIS [8]		✓			$N$ with RS <sup>†</sup>
Block Sampling [9]	✓	✓	✓		$LN$
Online Particle Smoother (Algorithm 4)	✓	✓	For large $L$	✓	$N^2$ $N$ with RS <sup>†</sup>
Online Particle Smoother with Backward Simulation (Algorithm 5)	✓	✓		✓	$LN^2$ $LN$ with RS <sup>†</sup>

Table 1: Comparison of smoothing algorithms, for number of particles  $N$  and fixed-lag parameter  $L$ .

<sup>†</sup>For these algorithms the rejection sampling technique of [10] can be applied to obtain linear complexity when a bound for the transition density (14) is available.

---

**Algorithm 1** Particle Filter

---

- 0: Input weighted sample  $\{x_{0:T-1}^{(i)}, w_{T-1}^{(i)}\}_{i=1}^N$  approximating  $p(x_{0:T-1}|y_{0:T-1})$  and new observation  $y_T$ .  
1: Resample (optional).

$$\left\{x_{0:T-1}^{(i)}, w_{T-1}^{(i)}\right\}_{i=1}^N \rightarrow \left\{x_{0:T-1}^{(i)}, \frac{1}{N}\right\}_{i=1}^N$$

- 2: Propagate by sampling from some proposal distribution.

$$x_T^{(i)} \sim q\left(x_T \mid x_{T-1}^{(i)}, y_T\right), \quad i = 1, \dots, N.$$

Append to particle  $x_{0:T}^{(i)} = (x_{0:T-1}^{(i)}, x_T^{(i)})$ .

- 3: Weight and normalise.

$$w_T^{(i)} \propto \frac{p\left(x_T^{(i)} \mid x_{T-1}^{(i)}\right) p\left(y_T \mid \tilde{x}_T^{(i)}\right)}{q\left(x_T^{(i)} \mid x_{T-1}^{(i)}, y_T\right)} w_{T-1}^{(i)} \quad i = 1, \dots, N.$$

- 4: Output weighted sample  $\{x_{0:T}^{(i)}, w_T^{(i)}\}_{i=1}^N$  approximating  $p(x_{0:T}|y_{0:T})$ .
-

The reason that a classical particle filter is almost never used to approximate the smoothing distribution is due to *path degeneracy*. Path degeneracy occurs in state-space models with large  $T$ . For repeated particle filter updates, the early coordinates of particles (e.g.  $x_0^{(i)}$ ) will only be altered in the resampling step. Resampling can only decrease particle diversity (the number of distinct particles) and therefore as  $T$  increases the particle approximation of  $p(x_0|y_{0:T})$  will eventually collapse to just a single particle duplicated  $N$  times.

## 2.2 Marginal Fixed-Lag

An intuitive approach to mitigate the path degeneracy induced by repeated resampling is to simply stop resampling the early coordinates of particles, as proposed in [4]. That is replace the resample step (Algorithm 1, step 1) for  $T > L$  with the scheme described in Algorithm 2.

---

**Algorithm 2** Marginal Fixed-lag Resampling (for  $T > L$ )

---

- 1: Fix  $\{x_{0:T-L-1}^{(i)}\}_{i=1}^N$
- 2: Resample only recent coordinates

$$\left\{x_{T-L:T}^{(i)}, w_T^{(i)}\right\}_{i=1}^N \rightarrow \left\{x_{T-L:T}^{(i)}, \frac{1}{N}\right\}_{i=1}^N$$

Stitch arbitrarily  $x_{0:T}^{(i)} = (x_{0:T-L-1}^{(i)}, x_{T-L:T}^{(i)})$ .

---

The justification for freezing  $x_{0:T-L-1}^{(i)}$  is that after a certain lag  $L$  the smoothing distribution of early instances become (approximately) independent of new observations

$$p(x_{0:t}|y_{0:T}) \approx p(x_{0:t}|y_{0:\min(t+L,T)}). \quad (2)$$

The major issue with the fixed-lag resampling scheme described in Algorithm 2 is that early and recent coordinates of particles are arbitrarily stitched together and therefore only provide a particle approximation to the *fixed-lag marginal* smoothing distribution:

$$p_{\text{marg}}^L(x_{0:T}|y_{0:T}) = \prod_{t=0}^{T-L-1} p(x_t|y_{0:t+L})p(x_{T-L:T}|x_{T-L-1}, y_{T-L:T}). \quad (3)$$

As such we lose information about the joint distribution of early coordinates  $x_{0:T-L-1}$ , despite being faithful to the fixed lag approximation (2).

A more useful particle approximation targets the *fixed-lag joint* smoothing distribution

$$p^L(x_{0:T}|y_{0:T}) = p(x_0|y_{0:L}) \prod_{t=1}^{T-L-1} p(x_t|x_{t-1}, y_{t:t+L})p(x_{T-L:T}|x_{T-L-1}, y_{T-L:T}), \quad (4)$$

which permits expectations over full trajectories  $x_{0:T}$ .

## 2.3 Offline Smoothing

A popular method for approximating the smoothing distribution  $p(x_{0:T}|y_{0:T})$  is that of *forward filtering-backward smoothing* [5]. This method stores the output of each particle

filter update and runs a full backward pass that updates the weights based on the backward decomposition

$$p(x_t|x_{t+1}, y_{0:t}) = \frac{p(x_{t+1}|x_t)p(x_t|y_{0:t})}{p(x_{t+1}|y_{0:t})}, \quad t = T-1, \dots, 0. \quad (5)$$

Similarly, *forward filtering-backward simulation* (FFBSi) [6] runs a full backward pass based on the same decomposition, but samples a new ancestor from the particle cloud (according to (5)) rather than only updating the weights and thus targets the joint smoothing distribution. Additionally, [10] showed that rejection sampling can significantly reduce the complexity of this pass in the case that  $p(x_t|x_{t-1})$  has a tractable upper bound. An implementation of backward simulation is described in the Appendix, Algorithm 6.

Both of these algorithms require a full backward pass in light of every new observation and therefore aren't suitable for online smoothing.

## 2.4 Online Smoothing

It was noted in [7] that the forward filtering-backward smoothing algorithm can be implemented in a single forward pass in the case of *additive functionals*, i.e. expectations of the form

$$\mathbb{E}_{p(x_{0:T}|y_{0:T})}[h(x_{0:T})] \quad \text{where} \quad h(x_{0:T}) = \sum_{t=0}^{T-1} \tilde{h}_t(x_t, x_{t+1}).$$

The PaRIS algorithm [8] combines this technique with rejection sampling to implement an efficient and cheap version of forward filtering-backward simulation in a single forward pass (for additive functionals).

Although it permits the implementation of these online algorithms, the requirement of additive functionals is very restrictive. Additionally, the forward only technique is *function specific*, i.e. it directly updates an approximation to the expected value of the additive functional  $h$ . Our approach induces a fixed-lag approximation but is suitable to be re-used over a range of functions that are defined on full state trajectories.

Block sampling [9] is an online method that targets the full smoothing distribution (1). Every time a new observation is received, the block sampling scheme discards the most recent coordinates (within lag  $L$ ) and re-proposes from an enlarged proposal distribution based on many more recent observations. Although this scheme does make use of a fixed-lag parameter, the weights and resampling still act on the full smoothing distribution (1). By moving a larger proportion of the trajectories, block sampling can (when combined with adaptive resampling schemes) mitigate but not avoid path degeneracy as resampling still takes place over full trajectories. Our proposed method builds on the block sampling approach by proposing blocks with a single coordinate overlap and then resampling in a way that targets the fixed-lag joint (4).

## 3 Fixed-lag Stitching

We consider the online case where we are given particles

$$\left\{ x_{0:T-1}^{(i)} \right\}_{i=1}^N \quad \text{approximating} \quad p^L(x_{0:T-1}|y_{0:T-1}), \quad (6)$$

and receive new observation  $y_T$ . We look to update the particle approximation to target the updated fixed-lag joint smoothing distribution

$$p^L(x_{0:T}|y_{0:T}) = p^L(x_{0:T-L-1}|y_{0:T-1})p(x_{T-L:T}|x_{T-L-1}, y_{T-L:T}). \quad (7)$$

The fixed-lag approximation implies the distribution of the early coordinates  $x_{0:T-L-1}$  remains unchanged due to the new observation. Thus we leave them fixed and sample a new block  $\tilde{x}_{T-L:T}$  before discarding the previous  $x_{T-L:T-1}$  of (6), as in block sampling [9].

Devising good conditional proposals for  $p(\tilde{x}_{T-L:T}|x_{T-L-1}, y_{T-L:T})$  is difficult for general state-space models. Instead we propose sampling from the partial smoothing distribution with single coordinate overlap

$$\left\{ \tilde{x}_{T-L-1:T}^{(j)} \right\}_{j=1}^N \text{ approximating } p(x_{T-L-1:T}|y_{0:T}). \quad (8)$$

Initially we assume we can generate samples directly from  $p(x_{T-L-1:T}|y_{0:T})$  to explain our importance sampling scheme, even though this is not possible for non-trivial state-space models. In Section 4 we then describe two efficient methods for sampling from  $p(x_{T-L-1:T}|y_{0:T})$  by recycling previously generated particles.

### 3.1 Stitching Weights

As in [9], we propose combining our samples from (6) and (8) to target an extended distribution

$$\begin{aligned} \pi(x_{0:T-1}, \tilde{x}_{T-L-1:T}|y_{0:T}) &= p^L(x_{0:T-L-1}|y_{0:T-1}) \\ & p(\tilde{x}_{T-L:T}|x_{T-L-1}, y_{T-L:T}) \\ & \lambda(\tilde{x}_{T-L-1}, x_{T-L:T-1}|x_{0:T-L-1}, \tilde{x}_{T-L:T}, y_{0:T}), \end{aligned} \quad (9)$$

only now with additional overlap variable  $\tilde{x}_{T-L-1}$ . The first two terms give the desired fixed-lag joint distribution (7) over the stitched trajectory  $x_{0:T-L-1}$  and  $\tilde{x}_{T-L:T}$ . The remaining  $\tilde{x}_{T-L-1}$  and  $x_{T-L:T-1}$  are discarded, thus leaving the  $\lambda$  term as a balancing distribution which we are free to choose.

The sampling distributions of  $x_{0:T-1}$  are given in (6) and  $\tilde{x}_{T-L-1:T}$  in (8). Therefore, under (9) we get importance weights

$$\begin{aligned} w_T &= \frac{\pi(x_{0:T-1}, \tilde{x}_{T-L-1:T}|y_{0:T})}{p^L(x_{0:T-1}|y_{0:T-1})p(\tilde{x}_{T-L-1:T}|y_{0:T})}, \\ &= \frac{p(\tilde{x}_{T-L:T}|x_{T-L-1}, y_{T-L:T}) \lambda(\tilde{x}_{T-L-1}, x_{T-L:T-1}|x_{0:T-L-1}, \tilde{x}_{T-L:T}, y_{0:T})}{p(\tilde{x}_{T-L:T}|\tilde{x}_{T-L-1}, y_{T-L:T}) p(\tilde{x}_{T-L-1}|y_{0:T})p(x_{T-L:T-1}|x_{T-L-1}, y_{T-L:T-1})}. \end{aligned} \quad (10)$$

Where the fixed-lag approximation implies that the sampling and target distribution of  $x_{0:T-L-1}$  align and therefore don't contribute to the weights.

The optimal choice of  $\lambda$  (that which minimises the variance of the importance weights [9, 11]) brings the weights back to the retained space  $x_{0:T-L-1}, \tilde{x}_{T-L:T}$

$$\begin{aligned} w_T^{\text{opt}} &= \frac{p(\tilde{x}_{T-L:T}|x_{T-L-1}, y_{T-L:T})}{p(\tilde{x}_{T-L:T}|y_{0:T})}, \\ &= \frac{p(\tilde{x}_{T-L}|x_{T-L-1}) p(y_{T-L:T}|y_{0:T-L-1})}{p(\tilde{x}_{T-L}|y_{0:T-L-1}) p(y_{T-L:T}|x_{T-L-1})}. \end{aligned}$$

These weights are intractable as we cannot evaluate  $p(\tilde{x}_{T-L}|y_{0:T-L-1})$  for non-trivial state-space models.

By choosing the following suboptimal  $\lambda$

$$\begin{aligned}\lambda(\tilde{x}_{T-L-1}, x_{T-L:T-1}|x_{0:T-L-1}, \tilde{x}_{T-L:T}, y_{0:T}) \\ = p(\tilde{x}_{T-L-1}|y_{0:T-L-1})p(x_{T-L:T-1}|x_{T-L-1}, y_{T-L:T-1}),\end{aligned}$$

we obtain tractable weights

$$\begin{aligned}w_T &= \frac{p(\tilde{x}_{T-L:T}|x_{T-L-1}, y_{T-L:T})}{p(\tilde{x}_{T-L:T}|\tilde{x}_{T-L-1}, y_{T-L:T})} \frac{p(\tilde{x}_{T-L-1}|y_{0:T-L-1})}{p(\tilde{x}_{T-L-1}|y_{0:T})} \\ &= \frac{p(\tilde{x}_{T-L}|x_{T-L-1})}{p(\tilde{x}_{T-L}|\tilde{x}_{T-L-1})} \frac{p(y_{T-L:T}|y_{0:T-L-1})}{p(y_{T-L:T}|x_{T-L-1})}.\end{aligned}$$

The second term is constant for fixed  $x_{T-L-1}$  and is thus absorbed into the normalising constant

$$\begin{aligned}\sum_{j=1}^N \frac{p(\tilde{x}_{T-L}^{(j)}|x_{T-L-1})}{p(\tilde{x}_{T-L}^{(j)}|\tilde{x}_{T-L-1}^{(j)})} &\approx \int \frac{p(\tilde{x}_{T-L}|x_{T-L-1})}{p(\tilde{x}_{T-L}|\tilde{x}_{T-L-1})} p(\tilde{x}_{T-L-1:T-L}|y_{0:T}) d\tilde{x}_{T-L-1:T-L} \\ &= \frac{p(y_{T-L:T}|x_{T-L-1})}{p(y_{T-L:T}|y_{0:T-L-1})}.\end{aligned}$$

In the above calculations we have used Bayes' theorem and the conditional independence structure of state-space models.

Therefore, in the case where the proposals are generated with accompanying weights  $\tilde{w}_T$

$$\left\{ \tilde{x}_{T-L-1:T}^{(j)}, \tilde{w}_T^{(j)} \right\}_{j=1}^N \text{ approximating } p(x_{T-L-1:T}|y_{0:T}), \quad (11)$$

the stitching weights simply become

$$w_T^{(i \rightarrow j)} \propto \frac{p(\tilde{x}_{T-L}^{(j)}|x_{T-L-1}^{(i)})}{p(\tilde{x}_{T-L}^{(j)}|\tilde{x}_{T-L-1}^{(j)})} \tilde{w}_T^{(j)}, \quad (12)$$

which are normalised in  $j$ .

The result is an  $N^2$  weighted particle approximation to the updated joint fixed-lag smoothing distribution (7)

$$p^L(x_{0:T-L-1}, \tilde{x}_{T-L:T}|y_{0:T}) \approx \sum_{i=1}^N \sum_{j=1}^N w_T^{(i \rightarrow j)} \delta_{(x_{0:T-L-1}^{(i)}, \tilde{x}_{T-L:T}^{(j)})} (x_{0:T-L-1}, \tilde{x}_{T-L:T}). \quad (13)$$

### 3.2 Resampling

In order to obtain a practical algorithm we look to resample the  $N^2$  particle approximation down to  $N$  particles.

The fact that the distribution of the earlier coordinates  $x_{0:T-L-1}^{(i)}$  hasn't changed motivates us to keep them fixed and for each one resample a descendent according to (13).

---

**Algorithm 3** Fixed-lag Stitching
 

---

- 0: Input unweighted sample  $\{x_{0:T-L-1}^{(i)}\}_{i=1}^N$  approximating  $p^L(x_{0:T-L-1}|y_{0:T-1})$ ,  
 weighted sample  $\{\tilde{x}_{T-L-1:T}^{(j)}, \tilde{w}_T^{(j)}\}_{j=1}^N$  approximating  $p(x_{T-L-1:T}|y_{0:T})$ , bound  
 $\rho \geq p(x_{T-L}|x_{T-L-1})$  and the maximum number of rejections to attempt  $R$ .  
 1: Calculate the non-interacting stitching weights and normalise in  $j$

$$\hat{w}_T^{(j)} \propto \frac{1}{p(\tilde{x}_{T-L}^{(j)}|\tilde{x}_{T-L-1}^{(j)})} \tilde{w}_T^{(j)} \quad j = 1, \dots, N.$$

- 2: **for**  $i = 1, \dots, N$  **do**  
 3:   **for**  $r = 1, \dots, R$  **do**  
 4:     Sample  $c^* \sim \text{Categorical}\left(\left\{\hat{w}_T^{(j)}\right\}_{j=1}^N\right)$   
 5:     Sample  $u \sim U(0, 1)$   
 6:     **if**  $u < p(\tilde{x}_{T-L}^{(c^*)}|x_{T-L-1}^{(i)})/\rho$  **then**  
 7:       Accept  $c^*$   
 8:       **break**  
 9:     **end if**  
 10:   **end for**  
 11: **if** a sample  $c^*$  was accepted **then**  
 12:   Set  $x_{T-L:T}^{(i)} = \tilde{x}_{T-L:T}^{(c^*)}$   
 13: **else**  
 14:   Calculate the stitching weights and normalise in  $j$

$$w_T^{(i \rightarrow j)} \propto \frac{p(\tilde{x}_{T-L}^{(j)}|x_{T-L-1}^{(i)})}{p(\tilde{x}_{T-L}^{(j)}|\tilde{x}_{T-L-1}^{(j)})} \hat{w}_T^{(j)} \quad j = 1, \dots, N.$$

- 15:   Sample  $c_i \sim \text{Categorical}\left(\left\{w_T^{(i \rightarrow j)}\right\}_{j=1}^N\right)$   
 16:   Set  $x_{T-L:T}^{(i)} = \tilde{x}_{T-L:T}^{(c_i)}$   
 17:   **end if**  
 18: **end for**  
 19: Output unweighted sample  $\{x_{0:T}^{(i)}\}_{i=1}^N$  approximating  $p^L(x_{0:T}|y_{0:T})$ .
-



This can be done directly at a computational complexity of  $O(N^2)$ . However, when a bound for the transition density is available

$$\rho \geq p(x_{T-L}|x_{T-L-1}) \quad \forall x_{T-L-1}, x_{T-L}, \quad (14)$$

we can utilise the rejection sampling approach of [10] to avoid calculating all the normalisation constants and bring the computational complexity down to  $O(N)$ . In practice, the rejection sampling is not always faster than the direct one. A pragmatic approach is the hybrid described in [12] where for each particle, up to  $R < N$  samples are proposed to the rejection sampler, if all are subsequently rejected the direct scheme is applied, thus setting  $R = 0$  recovers the direct scheme. The hybrid algorithm is described in Algorithm 3.

## 4 Sampling from $p(x_{T-L-1:T}|y_{0:T})$

We now describe two methods for sampling coordinates  $\tilde{x}_{T-L-1:T}$  in a way that is asymptotically unbiased for  $p(x_{T-L-1:T}|y_{0:T})$ , and can therefore be plugged into the fixed-lag stitching procedure.

### 4.1 Particle Filter

Recall the online setting where we have unweighted particles  $\{x_{0:T-1}^{(i)}\}_{i=1}^N$  approximating  $p^L(x_{0:T-1}|y_{0:T-1})$  and receive a new observation  $y_T$ .

Our first method is based on the fact that the particle approximation provided by a classical particle filter is asymptotically unbiased for the full joint smoothing distribution (1). Although this approximation deteriorates due to path degeneracy it may still be sufficient for sampling the desired later particles  $x_{T-L-1:T}$ .

Thus we propose applying the classical particle filter proposal and weighting steps to  $\{x_{0:T-1}^{(i)}\}_{i=1}^N$ , generating weighted particles  $\{x_{0:T}^{(i)}, \tilde{w}_T^{(i)}\}_{i=1}^N$ , before splitting the trajectories

$$\left\{x_{0:T}^{(i)}, \tilde{w}_T^{(i)}\right\}_{i=1}^N \rightarrow \left\{x_{0:T-L-1}^{(i)}\right\}_{i=1}^N \quad \text{and} \quad \left\{\tilde{x}_{T-L-1:T}^{(i)}, \tilde{w}_T^{(i)}\right\}_{i=1}^N,$$

where  $\tilde{x}_{T-L-1:T}^{(i)} = x_{T-L-1:T}^{(i)}$ . Under the fixed-lag approximation,  $x_{0:T-L-1}$  is conditionally independent of  $y_T$  and therefore the new weights don't need to apply to these earlier coordinates. Whereas the  $\{\tilde{x}_{T-L-1:T}^{(i)}, \tilde{w}_T^{(i)}\}_{i=1}^N$  are asymptotically unbiased for the desired sampling distribution  $p(x_{T-L-1:T}|y_{0:T})$  and can therefore be plugged into the stitching procedure (11). The coordinates  $x_{T-L-1}$  are duplicated to provide the overlap required for stitching.

The algorithm is described in Algorithm 4, and ends up being a relatively simple modification to classical particle filter where the resampling step is compulsory and altered to include the stitching probabilities in the weights (12).

When the transition bound (14) is available the complexity of the update remains  $O(N)$  or  $O(N^2)$  when the bound is unavailable.

### 4.2 Partial Backward Simulation

If the lag parameter  $L$  is chosen to be too large, the above mechanism will still suffer from path degeneracy in the same way a particle filter does. To remedy this we propose a partial run of the forward filtering-backward simulation [6, 10] (Algorithm 6) at each time step to

---

**Algorithm 4** Online Particle Smoother (for  $T > L$ )

---

0: Input unweighted smoothing sample  $\{x_{0:T-1}^{(i)}\}_{i=1}^N$  approximating  $p^L(x_{0:T-1}|y_{0:T-1})$ , new observation  $y_T$  and fixed-lag  $L$ .

1: Fix  $\{x_{0:T-L-1}^{(i)}\}_{i=1}^N$

2: Execute particle filter propagate and weight steps, Algorithm 1: steps 2-3

Generate  $\{\tilde{x}_{T-L-1:T}^{(j)}, \tilde{w}_T^{(j)}\}_{j=1}^N$  from  $\{x_{T-L-1:T-1}^{(j)}\}_{j=1}^N$  and  $y_T$ ,

forming a weighted sample approximating  $p(x_{T-L-1:T}|y_{0:T})$ .

3: Stitch together

$$\{x_{0:T-L-1}^{(i)}\}_{i=1}^N \text{ and } \{\tilde{x}_{T-L-1:T}^{(j)}, \tilde{w}_T^{(j)}\}_{j=1}^N \rightarrow \{x_{0:T}^{(i)}\}_{i=1}^N.$$

using Algorithm 3.

4: Output unweighted sample  $\{x_{0:T}^{(i)}\}_{i=1}^N$  approximating  $p^L(x_{0:T}|y_{0:T})$

---

rejuvenate the trajectories  $x_{T-L-1:T}$ . This technique is considered in [13] for generating samples from  $p(x_{T-L:T}|y_{0:T})$  without the subsequent stitching.

This has the additional requirement of storing the marginal particle filter approximations  $\{\tilde{x}_t^{(k)}, \tilde{w}_t^{(k)}\}_{k=1}^N$  for  $t = T-L-1, \dots, T$ , but permits the use of adaptive resampling in the particle filter and completely avoids path degeneracy.

The resulting algorithm, Algorithm 5, has a complexity of  $O(LN)$  per update if the transition bound (14) is available otherwise  $O(LN^2)$ .

## 5 Map-Matching

Map-matching is the task of inferring the true trajectory of a vehicle given noisy GPS observations and a map of the road network. A road network is defined as a graph in  $\mathbb{R}^2$ , where intersections are represented by nodes (vertices) and roads, which are assumed to be single lane and one-way, are represented by edges which preserve the possibly complex geometry of the road network (a two-way road is represented by two edges). Some collections of nodes and edges are depicted in Figure 2, 4 and 6, with map-matched vehicle routes overlaid.

Applications of map-matching are wide-ranging and thus a general purpose algorithm is highly desirable. Existing probabilistic approaches to map-matching have mostly adopted the approach of [14], where each observation is snapped to the nearest point on any and all edges that fall within a truncation distance. These points then form a discrete hidden Markov model, on which the Viterbi algorithm can produce a single route of high probability. In contrast, our approach provides uncertainty quantification through a collection of particles, with each particle representing a possible route. Previous applications of particle filtering to map-matching [15, 16] fail to tackle the problem of path degeneracy, with the exception of [17] who introduce the use of FFBSi for offline map-matching. Our formulation is similar to that of [17] but differs through the inclusion of a term in the transition density adapted from [14] that penalises non-direct routes, as well as the use of the optimal proposal density (that takes into account the new observation) rather than simply the bootstrap proposal which will perform poorly for small GPS noise or dense road networks.

In the rest of this section we describe our state-space model for map-matching, the

---

**Algorithm 5** Online Particle Smoother with Backward Simulation (for  $T > L$ )

---

- 0: Input unweighted smoothing sample  $\{x_{0:T-1}^{(i)}\}_{i=1}^N$  approximating  $p^L(x_{0:T-1}|y_{0:T-1})$ , weighted marginal filtering samples  $\{\tilde{x}_t^{(k)}, \tilde{w}_t^{(k)}\}_{k=1}^N$  for  $t = T-L-1, \dots, T-1$  each approximating  $p(x_t|y_{0:t})$ , new observation  $y_T$ , and fixed-lag  $L$ .
- 1: Fix  $\{x_{0:T-L-1}^{(i)}\}_{i=1}^N$
- 2: Execute particle filter update, Algorithm 1, to generate the new marginal filtering sample

$$\text{Generate } \{\tilde{x}_T^{(k)}, \tilde{w}_T^{(k)}\}_{k=1}^N \text{ from } \{\tilde{x}_{T-1}^{(k)}, \tilde{w}_{T-1}^{(k)}\}_{k=1}^N \text{ and } y_T.$$

- 3: Run partial backward simulation, Algorithm 6, on the weighted filtering samples

$$\{\tilde{x}_t^{(k)}, \tilde{w}_t^{(k)}\}_{k=1}^N, \text{ for } t = T, \dots, T-L-1 \rightarrow \{\tilde{x}_{T-L-1:T}^{(j)}\}_{j=1}^N.$$

forming an unweighted sample approximating  $p(x_{T-L-1:T}|y_{0:T})$ .

- 4: Stitch together

$$\{x_{0:T-L-1}^{(i)}\}_{i=1}^N \text{ and } \{\tilde{x}_{T-L-1:T}^{(j)}, \frac{1}{N}\}_{j=1}^N \rightarrow \{x_{0:T}^{(i)}\}_{i=1}^N.$$

using Algorithm 3.

- 5: Output unweighted sample  $\{x_{0:T}^{(i)}\}_{i=1}^N$  approximating  $p^L(x_{0:T}|y_{0:T})$  and weighted filtering samples  $\{\tilde{x}_T^{(k)}, \tilde{w}_T^{(k)}\}_{k=1}^N$ ,  $t = T-L, \dots, T$ .
- 

optimal proposal distribution and the induced weights in the context of fixed-lag stitching. In the next section we present some results on synthetic and real data. An open source python package providing easy offline and online map-matching is provided <sup>1</sup> alongside code for all the simulations to follow.

## 5.1 Model Variables

We define a state-space model for a single vehicle's trajectory with the variables

- $e_t \subset \mathbb{N}$ , a finite ordered set of connected edge labels, each edge label corresponds to a unique one-way section of road.  $e_t$  details the edges traversed (and in which order) between observation times  $t-1$  and  $t$ , including the choices made at encountered intersections (nodes).
- $x_t \in \mathbb{R}^2$  the position of the vehicle at observation time.  $x_t$  defines a Cartesian coordinate that is restricted to lie on the road network, specifically  $x_t$  lies on the final edge of the finite ordered set of edge labels  $e_t$ , for  $t > 0$ .
- $y_t \in \mathbb{R}^2$  noisy observation of the vehicle's position  $x_t$ , not restricted to the road network.

Note here the change of notation from the previous section, now  $x_t$  refers only to vehicle position and the full latent states are  $x_0, (e_1, x_1), (e_2, x_2), \dots, (e_T, x_T)$ , Figure 1.

We use the notation  $e(x_t)$  to denote the edge label of the edge on which  $x_t$  lies.

---

<sup>1</sup><https://github.com/SamDuffield/bmm>

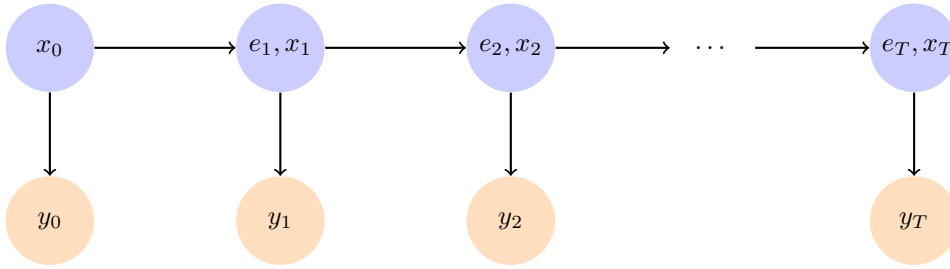


Figure 1: Conditional independence structure of the state-space model for map-matching.

## 5.2 Model Distributions

Our transition density can be written as

$$p(e_t, x_t | x_{t-1}) = \frac{\gamma(\|x_t - x_{t-1}\|_{e_t}) \exp(-\beta(\|x_t - x_{t-1}\|_{e_t} - \|x_t - x_{t-1}\|))}{Z(x_{t-1})}, \quad (15)$$

with normalising constant

$$Z(x_{t-1}) = \sum_{e_t} \int_{x_t} \gamma(\|x_t - x_{t-1}\|_{e_t}) \exp(-\beta(\|x_t - x_{t-1}\|_{e_t} - \|x_t - x_{t-1}\|)) dx_t, \quad (16)$$

where we always have the constraints  $e(x_{t-1}) = e_t^o$  (the first edge of  $e_t$ ) and  $e(x_t) = e_t^*$  (the last edge of  $e_t$ ). Recall that  $e_t$  is a finite ordered set of edge labels, starting with  $e_t^o$  and ending with  $e_t^*$ . The summation in (16) is taken over all possible series of edges starting at  $e(x_{t-1})$ .

$\|x_t - x_{t-1}\|_{e_t}$  is the distance travelled between  $x_{t-1}$  and  $x_t$  along the series  $e_t$  (restricted to the road network) whereas  $\|x_t - x_{t-1}\|$  is the *great circle* distance (not restricted to the road network).

Thus the following distributions fully define our state-space model:

- $\gamma(\|x_t - x_{t-1}\|_{e_t})$ . Prior on distance travelled between observations - some simple analytical distribution on  $\mathbb{R}^+$ , penalising lengthy routes. We assume an exponential distribution with probability mass at 0 to represent the possibility of the vehicle remaining stationary (due to traffic lights, heavy traffic etc)

$$\begin{aligned} \gamma(\|x_t - x_{t-1}\|_{e_t}) &= p^0 \mathbb{I}(\|x_t - x_{t-1}\|_{e_t} = 0) \\ &\quad + (1-p^0) \mathbb{I}(\|x_t - x_{t-1}\|_{e_t} > 0) \lambda \exp(-\lambda \|x_t - x_{t-1}\|_{e_t}). \end{aligned} \quad (17)$$

- $\exp(-\beta(\|x_t - x_{t-1}\|_{e_t} - \|x_t - x_{t-1}\|))$  adapted from [14], penalising non-direct (or winding) routes. Non-direct routes with lots of curvature will have a high discrepancy between the road distance travelled and great circle distance and thus will have a low probability under this term, reflecting a driver's preference to take short, direct routes where possible.
- $p(y_t | x_t) = \mathcal{N}(y_t | x_t, \sigma_{\text{GPS}}^2 I_2)$ . Isotropic Gaussian observation noise.
- We set  $p(x_0)$  to be uniform on the road network. I.e. no prior information on the start of the trajectory other than constricting it to the road network (as with all inferred positions).

To make  $p(x_0|y_0)$  tractable we define the initial observation density to be a truncated Gaussian:

$$p(y_0|x_0) \propto \mathcal{N}(y_0|x_0, \sigma_{\text{GPS}}^2 I_2) \mathbb{I}(\|y_0 - x_0\| < r_{\text{GPS}}),$$

giving

$$p(x_0|y_0) \propto \mathcal{N}(x_0|y_0, \sigma_{\text{GPS}}^2 I_2) \mathbb{I}(\|y_0 - x_0\| < r_{\text{GPS}}),$$

where  $x_0$  is restricted to the road network but  $y_0$  is not. In our simulations we set  $r_{\text{GPS}} = 5\sigma_{\text{GPS}}$ .

### 5.3 Optimal Proposal

The (locally) optimal proposal [18] for particle filtering combines the transition density (15) and the newly received observation  $y_T$ :

$$q^{\text{opt}}(x_T, e_T|x_{T-1}, y_T) \propto p(e_T, x_T|x_{T-1})p(y_T|x_T). \quad (18)$$

The standard reweighting step of the particle filter update (Algorithm 1) then becomes

$$w_T^{\text{opt}(i)} \propto p(y_T|x_{T-1}^{(i)}),$$

where

$$p(y_T|x_{T-1}) = \sum_{e_T} \int_{x_T} p(e_T, x_T|x_{T-1})p(y_T|x_T) dd_T, \quad (19)$$

is the normalisation constant of (18).

Neither sampling from the optimal proposal (18), nor evaluating the subsequent weights (19), nor evaluating the normalising constant of the transition density (16) are immediately tractable as we don't have closed form expressions for the edge geometries.

Instead, we opt to approximate the required integrals numerically by discretising the edges up to some maximal possible distance travelled  $d_{\text{max}}$ . This numerical integration can be implemented efficiently across particles by caching route searches and likelihood evaluations, as many particles will typically lie on the same or adjacent edges.

### 5.4 Fixed-lag Stitching

In the context of the fixed-lag stitching described in Section 3, we propose stitching together each

$$(x_{0:T-L-1}^{(i)}, e_{1:T-L-1}^{(i)}) \text{ with a sample from } \left\{ \tilde{x}_{T-L-1:T}^{(j)}, \tilde{e}_{T-L:T}^{(j)} \right\}_{j=1}^N.$$

Thus the adjusted weights become

$$w_T^{(i \rightarrow j)} \propto \frac{p(\tilde{e}_{T-L}^{(j)}, \tilde{x}_{T-L}^{(j)}|x_{T-L-1}^{(i)}) w_T^{(j)} \mathbb{I}(e(x_{T-L-1}^{(i)}) = \tilde{e}_{T-L}^{(j)})}{p(\tilde{e}_{T-L}^{(j)}, \tilde{x}_{T-L}^{(j)}|\tilde{x}_{T-L-1}^{(j)})}.$$

Similarly, for the rejection sampling we get non-interacting weights

$$\hat{w}_T^{(j)} \propto \frac{w_T^{(j)}}{p(\tilde{e}_{T-L}^{(j)}, \tilde{x}_{T-L}^{(j)}|\tilde{x}_{T-L-1}^{(j)})},$$

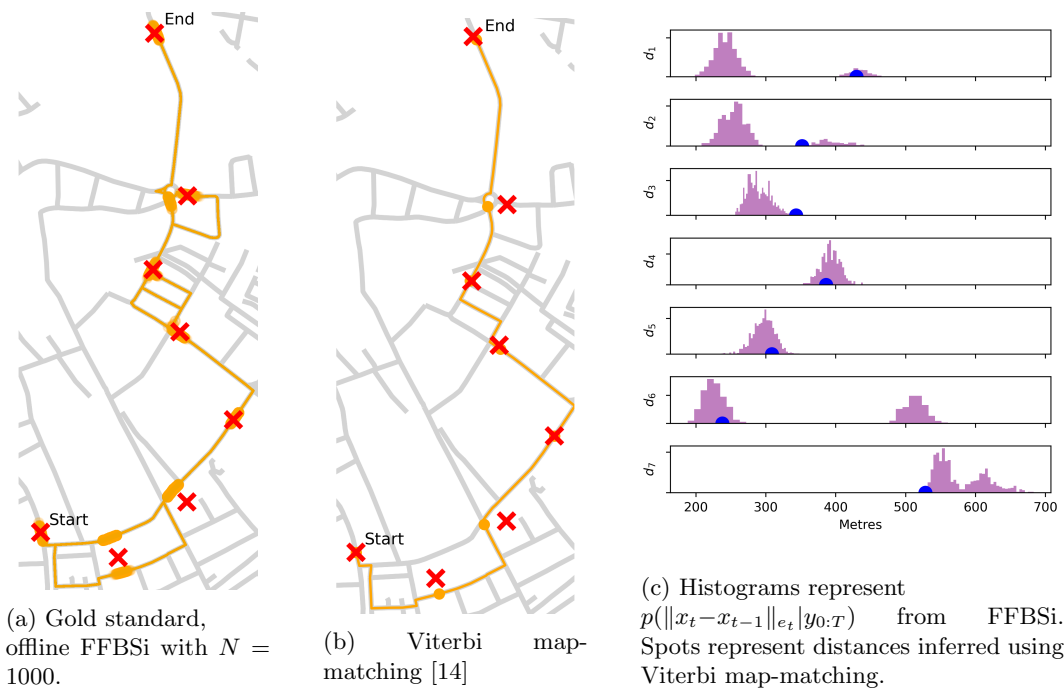


Figure 2: Offline particle smoothing vs Viterbi map-matching for synthetic trip across Cambridge.

and we accept a sample if  $e(x_{T-L-1}^{(i)}) = \tilde{e}_{T-L}^{(j)}$  and

$$u < \frac{\gamma\left(\|\tilde{x}_{T-L}^{(j)} - x_{T-L-1}^{(i)}\|_{\tilde{e}_{T-L}^{(j)}}\right) \exp\left(-\beta\left|\|\tilde{x}_{T-L}^{(j)} - x_{T-L-1}^{(i)}\|_{\tilde{e}_{T-L}^{(j)}} - \|\tilde{x}_{T-L}^{(j)} - x_{T-L-1}^{(i)}\|\right|\right)}{\rho},$$

where  $u \sim U(0, 1)$  and we have a bound  $\rho > \gamma(d)$  for any  $d$ . The availability of this bound depends on the choice of distribution for  $\gamma(\cdot)$ , in the case of (17) a bound is available:  $\rho = \max((1 - p^0)\lambda, p^0)$ .

## 6 Simulations

We tuned the model hyperparameters using offline gradient expectation-maximisation [19] (running offline FFBSi for the E-step) over 20 routes from the Porto taxi dataset [20] where observations are 15 seconds apart, resulting in values of  $p^0 = 0.14$ ,  $\lambda = 0.07/15$ ,  $\beta = 0.05$  and  $\sigma_{\text{GPS}} = 5.2$ , all edges are discretised to a resolution of 1m.

The true map-matching posterior is analytically intractable and instead we use an algorithmic *gold standard* for benchmarking: offline forward-filtering backward simulation with a large  $N = 1000$ , that is Algorithm 1 to generate the filtering marginals and Algorithm 6 for the smoothing particles.

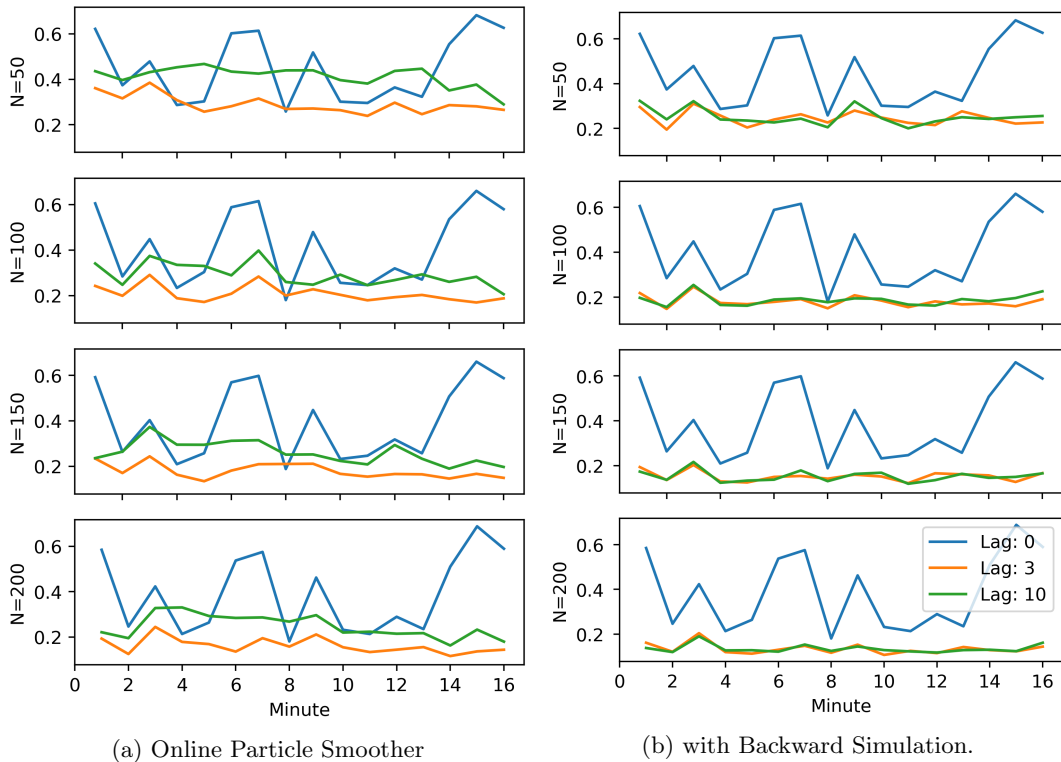


Figure 3: Total variation distance from gold standard (offline FFBSi) for distribution over cumulative distance travelled in each minute of a 16 minute taxi route (observation every 15 seconds) [20]. Simulations averaged over 20 random seeds.

## 6.1 Synthetic Data

In Figure 2 we demonstrate the benefits of uncertainty quantification for offline map-matching by comparing our particle based gold standard (offline FFBSi) with the popular optimisation approach of [14] on synthetic observations for a trip between the Cambridge Engineering department and the Fort St George pub.

## 6.2 Real Data

We now explore the effects of the algorithmic parameters in the online particle smoothers (sample size, lag parameter and number of rejections) for map-matching a route from the Porto taxi dataset [20], Figure 6.

In Figure 3, we analyse the posterior distribution for the cumulative (road) distance travelled by the taxi each minute. As observations are received every 15 seconds this amounts to expectations averaged over blocks of the full smoothing distribution and thus marginal approximations (3) would be insufficient. For each minute of the trip, we compare particle approximations by calculating the total variation distance over the empirical distributions (histograms). Figure 4 depicts the varying algorithmic performance on the start of the route.

We initially observe that setting  $L = 0$  performs very poorly for all sample sizes. The overly small lag parameter results in a large deviation between the true smoothing distribu-

tion (1) and the joint fixed-lag smoothing distribution (4), Figure 4b.

The online particle smoother suffers from path degeneracy for the large lag  $L = 10$  as observed by a loss of particle diversity (compared to the backward simulation techniques) in Figure 4c. It does however perform well for  $L = 3$ .

The addition of backward simulation avoids the issue of path degeneracy. We observe that increasing the lag parameter from  $L = 3$  to  $L = 10$  does little to improve performance and as such can posit that the distributions (1) and (4) are suitably close for  $L = 3$ , at least for the observations for this route, Figure 6.

Finally, in Figure 5 we compare the effect on algorithmic runtime from increasing the maximum number of rejections,  $R$ , attempted in the hybrid stitching scheme Algorithm 3, as well as backward simulation if applicable. Recall that setting  $R = 0$  recovers the full  $O(N^2)$  scheme. For a suitably large number of rejections the runtimes of both algorithms can be seen to increase linearly in  $N$ .

## 7 Discussion

In this work, we have developed techniques to efficiently approximate the full joint smoothing distribution (1) or rather the fixed-lag approximation to it (2) in an online setting, this is highly desirable as it permits the online estimation of a range functions that are defined over full trajectories or any subset thereof. The online particle smoother (Algorithm 4) comes at the same computational complexity as a classical particle filter, whereas the inclusion of backward simulation (Algorithm 5) negates the issue of path degeneracy (for more difficult models where a large lag parameter is required) at a linear increase in computational complexity that is necessary to tackle more difficult state-space models with long mixing times.

We formulated a state-space model that is specifically designed for urban map-matching and demonstrated the value of particle based uncertainty quantification versus established optimisation based approaches. We then showed that the performance of gold standard offline smoothing can be obtained with the online particle smoothers.

The linear computational complexity of both online fixed-lag techniques (as well as offline forward-filtering backward simulation) algorithms is achieved using rejection sampling [10] and thus requires a bound on the transition density. For some models this bound is unavailable or very poor, resulting in a return to quadratic complexity. In these settings, it is possible to utilise rejection control techniques [21] to attach weights at all rejection sampling steps and retain linear complexity. Here the bound is replaced with a pseudo-bound parameter that controls the trade-off between number of rejections and variance of the weights. Alternatively, the rejection sampling could be implemented with pseudo-bound and on the event the transition density exceeds the pseudo-bound, increase and restart the process until a full run without exceeding. This way the particles are unweighted and the pseudo-bound is adapted at each assimilation time, but could be expensive if the transition density is particularly complex. These techniques are also amenable to offline forward-filtering backward simulation.

The choice of  $L$  determines the distance between the distributions  $p^L(x_{0:T}|y_{0:T})$  and  $p(x_{0:T}|y_{0:T})$ , naturally we desire this to be small and thus  $L$  large. The question of how large is a difficult one as it is dependent on the mixing of the state-space model, as discussed in [8]. We have investigated the sensitivity of online smoothing to the choice of lag parameter for a particular instance of map-matching. An interesting extension would be to investigate the possibility of using a variable lag parameter which is chosen dynamically, as achieved





(a) Gold standard, offline FFBSi with  $N = 1000$ .



(b) Online particle smoother with  $L = 0$  and  $N = 200$ . Poor approximation due to small lag.



(c) Online particle smoother,  $L = 10$  and  $N = 200$ . Evidence of path degeneracy due to large lag.



(d) Online particle smoother with backward simulation,  $L = 10$  and  $N = 200$ .

Figure 4: The start of the route in Figure 6 with various particle approximations.

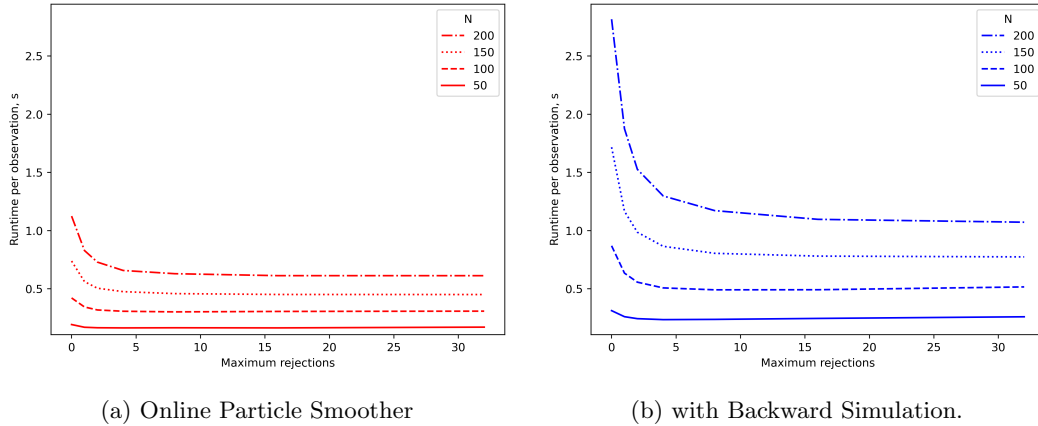


Figure 5: Algorithmic runtime vs number of rejections tolerated for  $L = 3$ . Runtimes averaged over 65 observations (Figure 6) and 20 random seeds.

for a function specific version of the marginal fixed-lag particle filter in [22].

The realisation of a low-probability transition or observation in the true underlying process can cause degeneracy either at stitching time or in the filtering weights. It is certainly possible to reintroduce particle diversity by applying an MCMC kernel after stitching as in resample-move particle filters [23] or particle rejuvenation [24]. The MCMC kernel is applied independently to each particle and must be invariant for the full smoothing distribution (1) but as we are only concerned with increasing particle diversity rather than taking ergodic averages we need only propose moving a subset of the trajectories, whether that be at stitching time or the latest observation time.



Figure 6: GPS observations for single taxi route [20].

---

**Algorithm 6** Backward Simulation

---

0: Input weighted marginal filtering samples  $\{\tilde{x}_t^{(k)}, \tilde{w}_t^{(k)}\}_{k=1}^N$  for  $t = 0, \dots, T$  each approximating  $p(x_t|y_{0:t})$ , bound  $\rho \geq p(x_t|x_{t-1})$  and the maximum number of rejections to attempt  $R$ .

1: Resample

$$\left\{ \tilde{x}_T^{(k)}, \tilde{w}_T^{(k)} \right\}_{k=1}^N \rightarrow \left\{ x_T^{(i)} \right\}_{i=1}^N$$

2: **for**  $t = T - 1, \dots, 0$  **do**

3:   **for**  $i = 1, \dots, N$  **do**

4:     **for**  $r = 1, \dots, R$  **do**

5:       Sample  $c^* \sim \text{Categorical} \left( \left\{ \tilde{w}_t^{(k)} \right\}_{k=1}^N \right)$

6:       Sample  $u \sim U(0, 1)$

7:       **if**  $u < p(x_{t+1}^{(i)}|\tilde{x}_t^{(c^*)})/\rho$  **then**

8:         Accept  $c^*$

9:         **break**

10:       **end if**

11:     **end for**

12:     **if** a sample  $c^*$  was accepted **then**

13:       Set  $x_t^{(i)} = \tilde{x}_t^{(c^*)}$

14:     **else**

15:       Calculate interacting weights and normalise in  $k$

$$w_t^{(k \leftarrow i)} \propto p(x_{t+1}^{(i)}|\tilde{x}_t^{(k)})\tilde{w}_t^{(k)} \quad k = 1, \dots, N.$$

16:       Sample  $c_i \sim \text{Categorical} \left( \left\{ w_t^{(k \leftarrow i)} \right\}_{k=1}^N \right)$  and set  $x_t^{(i)} = \tilde{x}_t^{(c_i)}$

17:     **end if**

18:   **end for**

19: **end for**

20: Output unweighted sample  $\left\{ x_{0:T}^{(i)} \right\}_{i=1}^N$  approximating  $p(x_{0:T}|y_{0:T})$ .

---

## References

- [1] N. Gordon, D. Salmond, and A. Smith, "Novel approach to nonlinear/non-gaussian bayesian state estimation," *IEEE Proceedings F, Radar and Signal Processing*, vol. 140, no. 2, pp. 107–113, 1993.
- [2] A. Doucet, N. d. Freitas, and N. Gordon, Eds., *Sequential Monte Carlo Methods in Practice*, ser. Information Science and Statistics. New York: Springer-Verlag, 2001. [Online]. Available: <https://www.springer.com/gb/book/9780387951461>

- [3] N. Chopin and O. Papaspiliopoulos, *An Introduction to Sequential Monte Carlo*, ser. Springer Series in Statistics. Springer International Publishing, 2020. [Online]. Available: <https://www.springer.com/gb/book/9783030478445>
- [4] G. Kitagawa and S. Sato, *Monte Carlo Smoothing and Self-Organising State-Space Model*. New York, NY: Springer New York, 2001, pp. 177–195. [Online]. Available: [https://doi.org/10.1007/978-1-4757-3437-9\\_9](https://doi.org/10.1007/978-1-4757-3437-9_9)
- [5] A. Doucet, S. Godsill, and C. Andrieu, “On sequential monte carlo sampling methods for bayesian filtering,” *Statistics and Computing*, vol. 10, 04 2003.
- [6] S. J. Godsill, A. Doucet, and M. West, “Monte carlo smoothing for nonlinear time series,” *Journal of the American Statistical Association*, vol. 99, no. 465, pp. 156–168, 2004. [Online]. Available: <https://doi.org/10.1198/016214504000000151>
- [7] P. Del Moral, A. Doucet, and S. S. Singh, “A backward particle interpretation of feynman-kac formulae,” *ESAIM: M2AN*, vol. 44, no. 5, pp. 947–975, 2010. [Online]. Available: <https://doi.org/10.1051/m2an/2010048>
- [8] J. Olsson and J. Westerborn, “Efficient particle-based online smoothing in general hidden markov models: The paris algorithm,” *Bernoulli*, vol. 23, no. 3, pp. 1951–1996, 08 2017. [Online]. Available: <https://doi.org/10.3150/16-BEJ801>
- [9] A. Doucet, M. Briers, and S. Sénécal, “Efficient block sampling strategies for sequential monte carlo methods,” *Journal of Computational and Graphical Statistics*, vol. 15, no. 3, pp. 693–711, 2006.
- [10] R. Douc, A. Garivier, E. Moulines, and J. Olsson, “Sequential monte carlo smoothing for general state space hidden markov models,” *The Annals of Applied Probability*, vol. 21, no. 6, pp. 2109–2145, 2011. [Online]. Available: <http://www.jstor.org/stable/41408080>
- [11] P. D. Moral, A. Doucet, and A. Jasra, “Sequential monte carlo samplers,” *Journal of the Royal Statistical Society. Series B (Statistical Methodology)*, vol. 68, no. 3, pp. 411–436, 2006. [Online]. Available: <http://www.jstor.org/stable/3879283>
- [12] E. Taghavi, F. Lindsten, L. Svensson, and T. B. Schön, “Adaptive stopping for fast particle smoothing,” in *2013 IEEE International Conference on Acoustics, Speech and Signal Processing*, 2013, pp. 6293–6297.
- [13] T. Clapp and S. Godsill, “Fixed-lag smoothing using sequential importance sampling,” 1999.
- [14] P. Newson and J. Krumm, “Hidden markov map matching through noise and sparseness,” in *Proceedings of the 17th ACM SIGSPATIAL International Conference on Advances in Geographic Information Systems*, ser. GIS ’09. New York, NY, USA: Association for Computing Machinery, 2009, p. 336–343. [Online]. Available: <https://doi.org/10.1145/1653771.1653818>
- [15] P. Davidson, J. Collin, and J. Takala, “Application of particle filters to a map-matching algorithm,” *Gyroscopy and Navigation*, vol. 2, no. 4, p. 285, Oct 2011. [Online]. Available: <https://doi.org/10.1134/S2075108711040067>

- [16] K. Kempinska, T. Davies, and J. Shawe-Taylor, “Probabilistic map-matching using particle filters,” *arXiv e-prints*, p. arXiv:1611.09706, Nov. 2016.
- [17] M. Roth, F. Gustafsson, and U. Orguner, “On-road trajectory generation from gps data: A particle filtering/smoothing application,” in *2012 15th International Conference on Information Fusion*, 2012, pp. 779–786.
- [18] A. Doucet, S. Godsill, and C. Andrieu, “On sequential Monte Carlo sampling methods for Bayesian filtering,” *Statistics and Computing*, vol. 10, no. 3, pp. 197–208, Jul. 2000. [Online]. Available: <https://link.springer.com/article/10.1023/A:1008935410038>
- [19] N. Kantas, A. Doucet, S. S. Singh, J. Maciejowski, and N. Chopin, “On particle methods for parameter estimation in state-space models,” *Statist. Sci.*, vol. 30, no. 3, pp. 328–351, 08 2015. [Online]. Available: <https://doi.org/10.1214/14-STS511>
- [20] L. Moreira-Matias, J. Gama, M. Ferreira, J. Moreira, and L. Damas, “Predicting taxi-passenger demand using streaming data,” *IEEE Transactions on Intelligent Transportation Systems*, vol. 14, pp. 1393–1402, 09 2013. [Online]. Available: <https://archive.ics.uci.edu/ml/datasets/Taxi+Service+Trajectory+-+Prediction+Challenge,+ECML+PKDD+2015>
- [21] J. S. Liu, R. Chen, and W. H. Wong, “Rejection control and sequential importance sampling,” *Journal of the American Statistical Association*, vol. 93, no. 443, pp. 1022–1031, 1998. [Online]. Available: <https://doi.org/10.1080/01621459.1998.10473764>
- [22] J. Alenlöv and J. Olsson, “Particle-based adaptive-lag online marginal smoothing in general state-space models,” *IEEE Transactions on Signal Processing*, vol. 67, no. 21, pp. 5571–5582, 2019.
- [23] W. R. Gilks and C. Berzuini, “Following a moving target—monte carlo inference for dynamic bayesian models,” *Journal of the Royal Statistical Society: Series B (Statistical Methodology)*, vol. 63, no. 1, pp. 127–146, 2001. [Online]. Available: <https://rss.onlinelibrary.wiley.com/doi/abs/10.1111/1467-9868.00280>
- [24] F. Lindsten, P. Bunch, S. S. Singh, and T. B. Schön, “Particle ancestor sampling for near-degenerate or intractable state transition models,” 2015.